





## Nanoscale patterning of polymers on DNA origami†

Nico Alleva, Pia Winterwerber, Colette J. Whitfield,  David Y. W. Ng \* and Tanja Weil\*Cite this: *J. Mater. Chem. B*, 2022, 10, 7512Received 13th April 2022,  
Accepted 4th June 2022

DOI: 10.1039/d2tb00812b

rsc.li/materials-b

The combination of DNA–origami and synthetic polymers paves the way to a new class of structurally precise biohybrid nanomaterials for diverse applications. Herein, we introduce the grafting to method with high conversions (70–90%) under ambient conditions to generate DNA–polymer conjugates, which can be hybridized precisely to DNA–origami architectures. We generated homo and block copolymers from three different polymer families (acrylates, methacrylates and acrylamides), coupled them to single stranded DNA (ssDNA) and pattern different DNA–origami architectures to demonstrate the formation of precise surface nanopatterns.

In recent years, DNA–polymer hybrid materials have received increasing interest as biosensors<sup>1</sup> or drug delivery systems.<sup>2</sup> Due to the high versatility of the synthetic polymer component,

a wide range of properties, particularly those that promote dynamic and responsive behaviour (*i.e.* pH, temperature), have been combined with the unique programmability offered by DNA nanotechnology.<sup>3</sup> DNA–polymer nanostructures have been realized and structure formations have been studied. One of the most elaborate examples exploits the polyanionic character of DNA with hydrophobic polymers to create amphiphilic conjugates that assemble into micelles.<sup>4</sup> Amphiphilic micelles have been made thermo-responsive by conjugation of the temperature-responsive polymer poly(*N*-isopropylacrylamide) (PNIPAM) and thus conferring its lower critical solution temperature (LCST) behaviour onto the eventual micelles.<sup>5</sup> These studies have since been expanded to include multi-responsiveness, not only from polymers, but also from oligonucleotides, such as the pH induced interconversion of “i-motif” structures.<sup>6</sup> In combination with the bioactivity of DNA–aptamer nanostructures, advanced drug delivery systems based on DNA–polymer conjugates have been developed.<sup>7</sup>

Importantly, the unique facet of DNA–polymer conjugates lies in a versatile platform to create architectures of higher complexity where DNA nanotechnology can be used to guide polymers with high precision in the nanoscale.<sup>8</sup> This strategy entails the use of DNA–origami as a template, where a long single-stranded (ss) DNA is folded by short oligonucleotides, so called staple strands, into complex 3-D DNA origami architectures like rectangles, tubes, stars or many other architectures.<sup>9</sup> As each grid position on DNA–origami can be independently functionalized, radical initiators<sup>10</sup> and/or photocatalysts<sup>11</sup> have been patterned to promote polymerization at the designated locations. However, conducting polymerization reactions directly on DNA–origami requires stringent conditions such as high ionic strength buffers with divalent cations Mg<sup>2+</sup>/Ca<sup>2+</sup>, low reaction volumes typically below 100 μl and mild reaction conditions during polymerization. This significantly limits both the monomer scope and polymerization technique. Additionally, it is often difficult to characterize the polymers (*i.e.* molecular weights, dispersity) grafted from the DNA origami due to its very low quantities. Herein, we circumvent these

Max Planck Institute for Polymer Research, Ackermannweg 10, 55128 Mainz, Germany. E-mail: david.ng@mpip-mainz.mpg.de, weil@mpip-mainz.mpg.de  
† Electronic supplementary information (ESI) available. See DOI: <https://doi.org/10.1039/d2tb00812b>



David Y. W. Ng

David received his BSc in Chemistry with first class honours in 2009 at the National University of Singapore. In 2010, his PhD studies on dendrimer–protein transporters was funded by the Max Planck Institute for Polymer Research (MPIP) to work under the supervision of Prof. Tanja Weil in Ulm. David graduated with summa cum laude in 2014 and led a junior group until 2016. He then moved to the MPIP and formed the synthetic life-like

systems group focusing on constructing dynamic bioactive structures in living cells. In 2021, he is appointed to concurrently lead the BioCore facility of the MPIP.



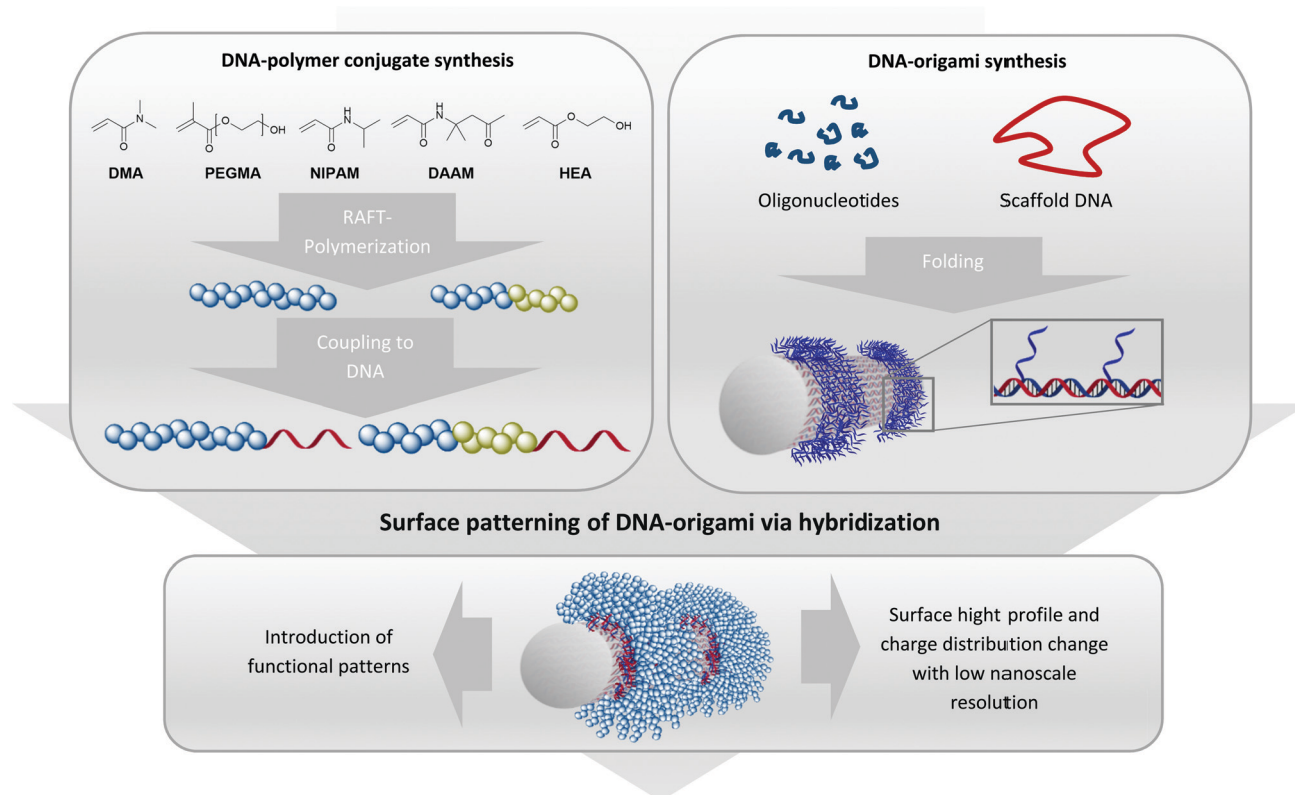


**Fig. 1** Concept of the combination of the grafting to method for generating DNA–polymer conjugates and the surface coating of DNA–origami due to protruding single stranded sticky sequences on the surface. The selected monomers form polymers with different features to diversify the inherent properties of DNA–origami nano-objects. The monomers were polymerized via RAFT polymerization and then coupled to single stranded DNA via NHS–amine conjugation chemistry under mild and ambient conditions. This versatile method generates a wide range of DNA–polymer conjugates for precise surface patterning of DNA–origami nanostructures.

limitations by adapting the grafting to approach, where polymers are synthesized in organic solvents (Fig. 1) before binding to DNA–origami for creating precise 3-D polymeric nanopatterns. This approach is already used in literature for the creation of functional DNA–polymer conjugates for *e.g.* fluorescent polythiophenes to form patterned DNA–origami in a high precise way.<sup>8,12</sup>

In order to position polymer chains onto DNA–origami, staple strands corresponding to the designated positions have to be elongated by a sticky DNA sequence. These extensions protrude as a ssDNA from the DNA–origami surface, allowing complementary sequences appended onto the polymer chains to recognize.<sup>13</sup> Hence, polymer chains with different sets of sticky DNA sequences can self-assemble onto their corresponding sites to afford a customizable architecture. As such, this technique grants access towards achieving precise geometric shapes that cannot be constructed *via* conventional polymer synthesis methods.<sup>14,15</sup> Three different kinds of monomer backbone (acrylates, methacrylates and acrylamides) were selected to underline the versatility of the approach. Technically, the production of 1–1 DNA–polymer conjugates can be performed *via* the grafting from or the grafting to method. In the grafting from method, the DNA block contains an initiator molecule and polymerization of the monomer proceeds *in situ*

to form the respective DNA–polymer conjugate.<sup>16</sup> However, the polymerization reaction has to be performed under conditions that accommodate the monomer, polymer and DNA components and there is a general loss of controllability and dispersity of the resultant polymers. On the contrary, the grafting to method synthesizes the polymer independently, which also facilitates characterization and easy scalability. After successful synthesis, bioconjugation to the DNA strand furnishes the target conjugate. As the polymer is synthesized prior the bioconjugation, the polymer block can be tailored with high flexibility even if the polymer chain is hydrophobic.<sup>17</sup> Due to these advantages, the grafting to method opens access to various DNA–polymer conjugates containing homo and block copolymers with hydrophilic and hydrophobic monomer units.<sup>18</sup>

Dimethyl acrylamide (DMA), oligoethylene glycol acrylate (OEGMA), *N*-isopropyl acrylamide (NIPAM), hydroxyethyl acrylate (HEA) and diacetone acrylamide (DAAM) were polymerized *via* reversible–addition–fragmentation chain-transfer polymerization (RAFT) to form the homo polymers and block copolymers (Fig. 2a). These monomers constitute widely used classes in the polymer community with DMA and OEGMA promoting aqueous solubility<sup>19</sup> whereas NIPAM, HEA and DAAM are common functional monomers in self-assembly systems.<sup>16,20</sup>





**Fig. 2** (a) Obtained polymers after CTA group removal, containing the NHS group for bioconjugation to DNA. (b) GPC traces of the NHS polymers P1–P8 as measured by DMF GPC using polymethylmethacrylate (PMMA) as calibration standard. (c) Schematic representation of the coupling reaction of the generated NHS polymers with the 5' amino oligonucleotide using DIPEA as the auxiliary base. (d) DNA and DNA–polymer conjugation reaction solutions analysed by 15% PAGE, stained with SYBR Gold. Complementary rhodamine DNA was used for hybridization to obtain better staining. L: DNA ladder; DNA: used 5' amino oligonucleotide; CP1–CP8: coupling reaction solutions of P1–P8 with 5' amino oligonucleotide (StA).

As with RAFT polymerization, the control over dispersity and chain length can be accomplished along with a wide selection of monomers and flexible end group modifications.<sup>16,21</sup> Polymerizations of DMA, NIPAM, HEA and DAAM were performed with 2-(dodecylthiocarbonothioylthio)-2-methylpropionic acid *N*-hydroxysuccinimide ester (NHS-DDMAT) acting as the chain transfer agent (CTA) in dioxane or DMF. Block co-polymerization consisting of hydrophobic P(DAAM) and hydrophilic P(DMA) were synthesized to demonstrate the robustness of the functionalization reaction and subsequent patterning. To prevent side reactions during the subsequent bioconjugation reaction with oligonucleotides, the CTA group of the NHS-polymers was removed post polymerization with an excess of azobisisobutyronitrile (AIBN) in dioxane at 75 °C. The obtained NHS-polymers revealed narrow molecular weight distributions ( $D = 1.08$ – $1.27$ , Table S3, ESI<sup>†</sup>) and a wide range of polymers with different molecular weights were synthesized (9.6–48.6 kDa, analysed by GPC (Fig. 2(b)). To perform the bioconjugation reaction of the NHS-functionalized polymers with the 5' amino oligonucleotide (complementary sticky A (StA<sup>C</sup>; 5'-NH<sub>2</sub>-TTTTCTCT ACCACTACTA-3')<sup>13</sup> or complementary sticky E (StE<sup>C</sup>; 5'-NH<sub>2</sub>-CAGTCAGTCAGTCAGTCAGT-3')<sup>15</sup>) (Fig. 2(c)), the solvent has a high impact on the conversion. The accessibility of the reactive

functionalities drives the reaction efficiency and therefore requires a good solvent that prevents aggregation of the polymer and the oligonucleotide chains. Optimization on the solvent conditions was performed in acetonitrile (ACN), dimethylformamide (DMF), water and mixtures thereof using **P2** as a model polymer, monitored by native polyacrylamide gel electrophoresis (PAGE) (Fig. S2 and S3, ESI<sup>†</sup>). In comparison, DMF:water (3:1) was the best reaction solvent to afford a conversion between 70–90% (Fig. 2d), quantified by integrating the band intensity of the PAGE gels (Fig. S1 and Table S2, ESI<sup>†</sup>). The PAGE revealed that the conversion depends on the chain length of the respective polymer, which is exemplarily shown for the DMA polymers (**P1–P3**) with increasing intensity of the unreacted 5' amino oligonucleotide. Comparing across polymer families, P(NIPAM-*b*-DMA) (**P6**) showed higher conversions than P(DMA) (**P2–P3**) and even the functionalization of P(OEGMA) (**P4**) proceeds well despite its brush like structure. Importantly, the reaction conditions were also robust for amphiphilic type block copolymer P(DAAM-*b*-DMA) **P8**, with an estimated conversion of ~90%.

Next, the DNA–polymer conjugates were patterned onto the surface of DNA origami nanotubes. First, the DNA–DMA conjugates of three different polymer chain length (**P1**: 9.6 kDa; **P2**:





**Fig. 3** (a) Schematic representation of the DNA–origami coating with DNA–polymer conjugates by hybridization at 37 °C. (b) Height changes of the DNA origami surface obtained *via* AFM, where the respective uncoated and the coated sections on the origami nanostructures were measured to obtain the height difference ( $n = 10$  times for each coating). Heights from Fig. S5–S8 and Tables S4–S7. (c) Uncoated DNA–origami imaged by AFM. Scale bar = 80 nm. (d) DNA–origami coated with CP3 imaged by AFM. Scale bar = 80 nm. (e) Monitoring of the coated and uncoated DNA–origami tube and rectangle containing StA by 1% agarose gel, stained with SYBR Gold; L: DNA ladder;  $O_4$ : uncoated DNA–origami;  $O_5$ : coated DNA–origami with CP3;  $O_6$ : uncoated DNA–origami;  $O_7$ : coated DNA–origami with CP2. (f–i) Respective DNA–origami architectures uncoated and coated with the respective DNA–polymer conjugate; tube: CP3; rectangle: CP2. Scale bar = 120 nm.

22.1 kDa; **P3**: 48.6 kDa), were purified *via* spin filtration to remove unreacted amino oligonucleotides. Subsequently, the conjugates were hybridized to the DNA–origami tube containing patterned StA sequences (Fig. 3a). The attachment was performed in origami buffer (1 mM  $\text{Na}_2\text{EDTA}$ , 5 mM NaCl, 5 mM Tris, 12 mM  $\text{MgCl}_2$  pH 8) at 37 °C for 1 h. The resulting architectures ( $O_1$ ,  $O_2$ ,  $O_3$ ) were monitored *via* atomic force microscopy (AFM) to determine the height profile of the DNA coated DNA–origami against uncoated DNA–origami ( $O_0$ ) (Fig. 3b). The increase in height as a function of polymer weight demonstrated successful hybridization of the polymer chains

and showed a nonlinear dependence between polymer length and height change. The trend is expected due to the increase in chain collapse as the molecular weight of the polymer chains increases. As such, the  $z$ -axis contribution per monomer is weighted less as the polymer grows larger. The attachment of the polymers was independently characterized using agarose gel, with shifts in molecular weight to charge ratios corresponding to the size of the polymers used (Fig. S4, ESI†).

To show the flexibility to accommodate patterns of varying shapes and of different origami templates, a DNA–origami tube containing four StA rings ( $O_4$ ) and a DNA–origami tile with two



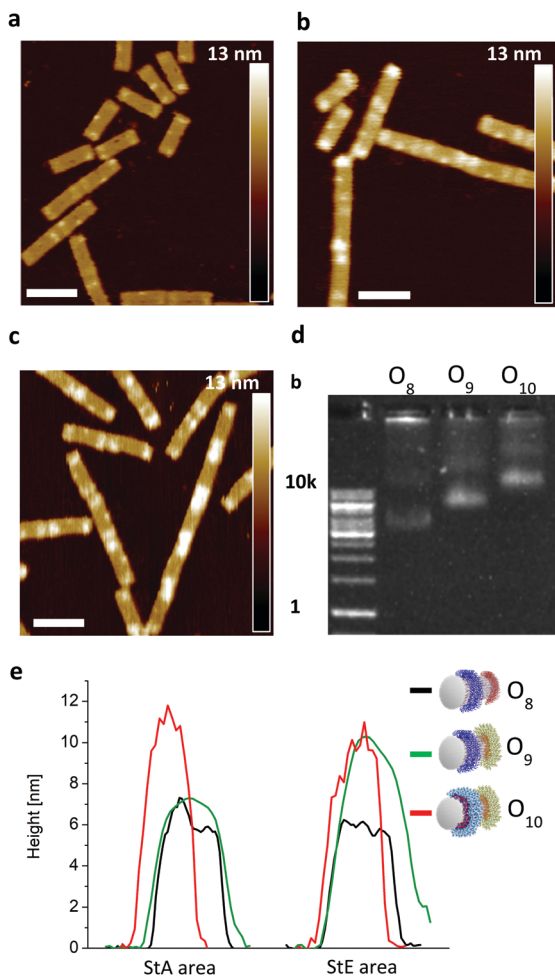


**Fig. 4** (a) Uncoated DNA-origami ( $O_8$ ) monitored *via* AFM. Scale bar = 100 nm (b) DNA-origami ( $O_9$ ) with  $StE^c$ -P7 monitored *via* AFM. Scale bar = 100 nm (c) DNA-origami ( $O_{10}$ ) coated with  $StE^c$ -P7 and CP2. Scale bar = 100 nm (d) Coated and uncoated DNA-origami monitored with 1% agarose gel, stained with SYBR Gold.  $O_8$  is uncoated,  $O_9$  is coated with  $StE^c$ -P7 and  $O_{10}$  is coated with CP2 and  $StE^c$ -P7. (e) AFM topographic images reveal a significant increase in height of the respective coating area.

StA triangles ( $O_6$ ) were hybridized with CP2 or CP3 and imaged *via* AFM (Fig. 3f–i). The topological height change observed in the AFM image and the band shift in the agarose gel (Fig. 3e) indicate that the patterning of the polymeric architectures was successful, demonstrating the nanoscale resolution of the coating, even for larger ( $\sim 50$  kDa) DNA-polymer conjugates. Further customization can be achieved by using different sticky sequences to assemble different polymers onto a single nano-object. A DNA-origami tube patterned with StE and StA sequences ( $O_8$ ) was hybridized with  $StE^c$ -P7 conjugate and CP2 (Fig. 4). The recognition between each set of sticky sequences and their complementary binding partners was characterized stepwise. Using  $O_8$ , hybridization was performed with  $StE^c$ -P7 to form  $O_9$ . The attachment of  $StE^c$ -P7 was observed *via* AFM only on one end of the DNA-origami tube resulting in a height difference of  $\sim 3$ –4 nm (Fig. 4e), thus

underlining the specificity of the hybridization reaction. The influence of the attached polymers in terms of molecular weight and charge change of the DNA-origami were determined by agarose gel electrophoresis (Fig. 4d). With both  $StE^c$ -P7 and CP2 present, the designated two-ring structure was formed.

Collectively, we showed that the grafting to strategy present several advantages over the grafting from strategy. First, the polymers can be fully characterized prior to patterning. This allows us to attribute material characteristics to each polymer scaffold and composition. In addition, the methodology is more modular, where polymer combinations one origami can be easily achieved. Furthermore, the grafting to strategy showed better sustainability and cost effectiveness evaluated by Eco Scale,<sup>22</sup> a green metric factor (see ESI†).

In conclusion, we have introduced a robust grafting to procedure under ambient conditions with high conversions to achieve various DNA-polymer conjugates containing homo and block copolymers. These DNA-polymer conjugates from widely used polymer families (methacrylates acrylates and acrylamides) show conserved DNA-based recognition properties to their complementary sequences. The hybridization process was also not affected by the steric demand of the polymer chain, which was demonstrated by varying the molecular weight from  $\sim 10$  kDa to 50 kDa. The attachment of the polymers to the DNA-origami was demonstrated on both tube and tile origamis. Different polymer chains, each equipped with a unique set of sticky sequences, can be attached onto each origami nano-object in a convenient manner also applicable for non-polymer chemists. With the rising importance of precisely engineered interfaces in nanotechnology and biomedicine, hybrid DNA-polymer conjugates remain one of the most accessible strategies to achieve coatings with nanoscale precision.

## Conflicts of interest

There are no conflicts to declare.

## Acknowledgements

The authors acknowledge the financial support by the Deutsche Forschungsgemeinschaft (DFG, German Research Foundation) – Project No. 364549901 – TRR 234 CataLight (B01) and the Max Planck Society for Open Access Funding.

## References

- 1 J. M. Gibbs, S.-J. Park, D. R. Anderson, K. J. Watson, C. A. Mirkin and S. T. Nguyen, *J. Am. Chem. Soc.*, 2005, **127**, 1170–1178.
- 2 H. Kang, H. Liu, X. Zhang, J. Yan, Z. Zhu, L. Peng, H. Yang, Y. Kim and W. Tan, *Langmuir*, 2011, **27**, 399–408.
- 3 (a) F. E. Alemendaroglu, K. Ding, R. Berger and A. Herrmann, *Angew. Chem., Int. Ed.*, 2006, **45**, 4206–4210; (b) F. Cavalieri, A. Postma, L. Lee and F. Caruso, *ACS Nano*, 2009, **3**, 234–240.



- 4 T. R. Wilks, J. Bath, J. W. de Vries, J. E. Raymond, A. Herrmann, A. J. Turberfield and R. K. O'Reilly, *ACS Nano*, 2013, **7**, 8561–8572.
- 5 K. Isoda, N. Kanayama, M. Fujita, T. Takarada and M. Maeda, *Chem. – Asian J.*, 2013, **8**, 3079–3084.
- 6 Z. Zhao, L. Wang, Y. Liu, Z. Yang, Y.-M. He, Z. Li, Q.-H. Fan and D. Liu, *Chem. Commun.*, 2012, **48**, 9753–9755.
- 7 L. Yang, H. Sun, Y. Liu, W. Hou, Y. Yang, R. Cai, C. Cui, P. Zhang, X. Pan, X. Li, L. Li, B. S. Sumerlin and W. Tan, *Angew. Chem., Int. Ed.*, 2018, **130**, 17294–17298.
- 8 J. B. Knudsen, L. Liu, A. L. Bank Kodal, M. Madsen, Q. Li, J. Song, J. B. Woehrstein, S. F. J. Wickham, M. T. Strauss, F. Schueder, J. Vinther, A. Krissanaprasit, D. Gudnason, A. A. A. Smith, R. Ogaki, A. N. Zelikin, F. Besenbacher, V. Birkedal, P. Yin, W. M. Shih, R. Jungmann, M. Dong and K. V. Gothelf, *Nat. Nanotechnol.*, 2015, **10**, 892–898.
- 9 P. W. K. Rothmund, *Nature*, 2006, **440**, 297–302.
- 10 Y. Tokura, Y. Jiang, A. Welle, M. H. Stenzel, K. M. Krzemien, J. Michaelis, R. Berger, C. Barner-Kowollik, Y. Wu and T. Weil, *Angew. Chem., Int. Ed.*, 2016, **128**, 5786–5791.
- 11 P. Winterwerber, S. Harvey, D. Y. W. Ng and T. Weil, *Angew. Chem., Int. Ed.*, 2020, **59**, 6144–6149.
- 12 J. Zessin, F. Fischer, A. Heerwig, A. Kick, S. Boye, M. Stamm, A. Kiriy and M. Mertig, *Nano Lett.*, 2017, **17**, 5163–5170.
- 13 P. Winterwerber, C. J. Whitfield, D. Y. W. Ng and T. Weil, *Angew. Chem., Int. Ed.*, 2021, e202111226.
- 14 N. P. Agarwal, M. Matthies, F. N. Gür, K. Osada and T. L. Schmidt, *Angew. Chem., Int. Ed.*, 2017, **56**, 5460–5464.
- 15 J. Schill, B. J. H. M. Rosier, B. Gumí Audenis, E. Magdalena Estirado, T. F. A. de Greef and L. Brunsveld, *Angew. Chem., Int. Ed.*, 2021, **60**, 7612–7616.
- 16 T. Lückerrath, K. Koynov, S. Loescher, C. J. Whitfield, L. Nuhn, A. Walther, C. Barner-Kowollik, D. Y. W. Ng and T. Weil, *Angew. Chem., Int. Ed.*, 2020, **59**, 15474–15479.
- 17 S. Hansson, V. Trouillet, T. Tischer, A. S. Goldmann, A. Carlmark, C. Barner-Kowollik and E. Malmström, *Biomacromolecules*, 2013, **14**, 64–74.
- 18 M. Safak, F. E. Alemdaroglu, Y. Li, E. Ergen and A. Herrmann, *Adv. Mater.*, 2007, **19**, 1499–1505.
- 19 (a) S. Maiez-Tribut, J. P. Pascault, E. R. Soulé, J. Borrajo and R. J. J. Williams, *Macromolecules*, 2007, **40**, 1268–1273; (b) K. G. Neoh and E. T. Kang, *Polym. Chem.*, 2011, **2**, 747–759.
- 20 A. Khan, T. H. Khan, A. M. El-Toni, A. Aldalbahi, J. Alam and T. Ahamad, *Mater. Lett.*, 2019, **235**, 197–201.
- 21 S. Goldmann, D. Quémener, P.-E. Millard, T. P. Davis, M. H. Stenzel, C. Barner-Kowollik and A. H. Müller, *Polymer*, 2008, **49**, 2274–2281.
- 22 K. Aken, L. Streckowski and L. Patiny, *Beilstein J. Org. Chem.*, 2006, **2**, 3.

